Heterometallic Cages

Deutsche Ausgabe: DOI: 10.1002/ange.201501041
Internationale Ausgabe: DOI: 10.1002/anie.201501041

$[Cr^{III}_8M^{II}_6]^{12+}$ Coordination Cubes (M^{II} = Cu, Co)**

Sergio Sanz, Helen M. O'Connor, Eufemio Moreno Pineda, Kasper S. Pedersen, Gary S. Nichol, Ole Mønsted, Høgni Weihe, Stergios Piligkos, Eric J. L. McInnes,* Paul J. Lusby,* and Euan K. Brechin**

Abstract: *$[Cr^{III}_8M^{II}_6]^{12+}$ (M^{II} = Cu, Co) coordination cubes were constructed from a simple $[Cr^{III}L_3]$ metalloligand and a "naked" M^{II} salt. The flexibility in the design proffers the potential to tune the physical properties, as all the constituent parts of the cage can be changed without structural alteration. Computational techniques (known in theoretical nuclear physics as statistical spectroscopy) in tandem with EPR spectroscopy are used to interpret the magnetic behavior.*

Molecules containing exchange-coupled paramagnetic metal ions represent a class of materials with potential applications across a breadth of scientific disciplines, with particular recent focus on information storage, quantum computation, and molecular spintronics.[1–6] The bottom-up design of magnetic materials for such applications is attractive, as molecules are inherently monodisperse, reproducible, orientable, and chemically tuneable. Synthetic strategies that target magnetic coordination compounds span the entire spectrum from the serendipitous self-assembly of coordinatively flexible metal ions and organic ligands capable of bridging in multiple ways, through to the design of structurally predictable cages using rigid linker ligands in combination with metal precursors that possess a limited number of coordination sites free for reaction.[7] This 'rational design' strategy has also been widely utilized for the preparation of numerous diamagnetic coordination capsules, the interest in these systems stemming from host–guest chemistry that has been exploited for catalysis, drug delivery, or the stabilization of reactive intermediates.[8] Heterometallic coordination capsules have also been accessed using preprogrammed self-assembly approaches, occasionally using one-pot, self-sorting strategies with thermodynamically orthogonal metal–ligand motifs,[9] or more commonly through a stepwise approach that takes advantage of kinetically robust intermediate complexes that possess pendant donor tectons, often referred to as metalloligands.[10–15] However, only a handful of these heterometallic systems possess paramagnetic centers,[13] and even fewer have been reported to display intramolecular magnetic exchange.[15]

Herein we discuss the structures and magnetic properties of the heterometallic cages $[Cr^{III}_8Cu^{II}_6L_{24}(H_2O)_{10}(NO_3)_2](NO_3)_{10}$ (**1**) and $[Cr^{III}_8Co^{II}_6L_{24}(H_2O)_{12}](ClO_4)_{12}$ (**2**), which were built using the simple metalloligand $[Cr^{III}L_3]$ (HL = 1-(4-pyridyl)butane-1,3-dione) and the metal salts $Cu(NO_3)_2\cdot 3H_2O$ and $Co(ClO_4)_2\cdot 6H_2O$, respectively. The metallic skeleton of both cages (Figure 1, see also Figures S1 and S2 in the Supporting Information) describes a simple $[Cr^{III}_8M^{II}_6]^{12+}$ cube with the Cr^{III} ions of the $[Cr^{III}L_3]$ metalloligands occupying the corners of the cube, and the M^{II} ions capping the square faces. The former are six-coordinate and in regular

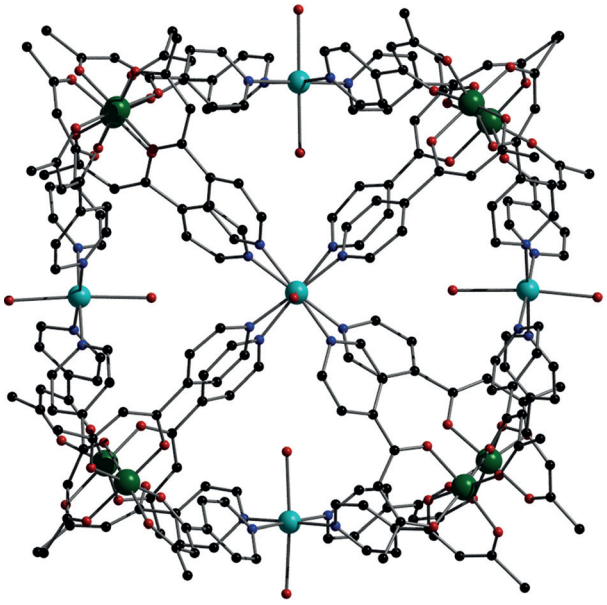

Figure 1. Molecular structure of the cation of **1**. Color code: Cr = green, Cu = light blue, O = red, N = blue, C = black. The terminally bound oxygen atoms originate from both water and nitrate molecules (see text for details).

[*] Dr. S. Sanz, H. M. O'Connor, Dr. G. S. Nichol, Dr. P. J. Lusby, Prof. E. K. Brechin
EaStCHEM School of Chemistry, The University of Edinburgh
David Brewster Road, Edinburgh, EH9 3FJ (UK)
E-mail: Paul.Lusby@ed.ac.uk
E.Brechin@ed.ac.uk
E. M. Pineda, Prof. E. J. L. McInnes
School of Chemistry, The University of Manchester
Oxford Road, Manchester M13 9PL (UK)
E-mail: eric.mcinnes@manchester.ac.uk
Dr. K. S. Pedersen, Dr. O. Mønsted, Dr. H. Weihe, Dr. S. Piligkos
Department of Chemistry, University of Copenhagen
Universitetsparken 5, 2100 Copenhagen (Denmark)
E-mail: piligkos@kiku.dk

[**] The authors acknowledge the EPSRC for funding, including the National EPR Facility at Manchester. S.P. thanks the Danish Ministry of Science, Innovation and Higher Education for a Sapere Aude Fellowship (10-081659).

Supporting information for this article is available on the WWW under http://dx.doi.org/10.1002/anie.201501041.

{CrO_6} octahedral geometry, with Cr–O distances between 1.88–2.04 Å, and *trans* angles in the range 175–179°. In **1**, the Cu^{II} ions are also six coordinate, but in Jahn–Teller distorted {CuN_4O_2} coordination geometries (Cu-N, ≈2 Å) with the O-Cu-O vector (Cu-O, ≈2.31–2.58 Å) describing the elongated axis (d_{z^2}), perpendicular to the equatorial CuN_4 plane ($d_{x^2-y^2}$) in the face of the cube. Ten of these axial ligands are H_2O molecules, but two (on opposing sides of the cube) are NO_3^- anions. In the extended structure (Figure S2), these link to neighboring cages, which results in the formation of a square sheet of cubes in the *bc* plane. The remaining ten, nonbonded, charge-balancing NO_3^- anions, and solvent molecules of crystallization, are located both within the cage cavity and in the void spaces between the cubes.

In complex **2** (Figure S1) the face-capping Co^{II} ions possess the same, albeit regular, octahedral {CoN_4O_2} geometry with Co–O bonds in the range 2.04–2.12 Å. Here, all the terminally coordinated ligands are water molecules. In the solid state, the cations of **2** pack in a brickwork-like fashion (Figure S3) with the closest intercage contacts being between the corners of neighboring cubes through a plethora of close contacts, primarily mediated by the L ligands: CH···O, ≈3.1 Å; CH_3···π, ≈3.6 Å; CH_3···CH, ≈4.0 Å; O···O, 4.3 Å; CH_3···CH_3, 4.5 Å. The twelve charge-balancing ClO_4^- anions, and solvent molecules of the crystallization, are again located both within the cage cavity and in the void spaces between cubes. The Cr···Cr distance between nearest neighbors along each edge of the cubes measures approximately 12 Å, creating an internal cavity volume close to 1000 $Å^3$ (Figure S4), thus suggesting that anions with a total volume of around 550 $Å^3$ could be accommodated.[11] Future studies will examine potential host–guest chemistry as a means of creating multifunctionality and additional magnetic exchange. The analogous diamagnetic $[Al^{III}_8Pd^{II}_6]^{12+}$ cage has been reported previously,[12] though its lack of solubility precluded the investigation of any host–guest chemistry, while similar structure types, albeit with different ligands, have been observed in the complex $[Cu^{II}_6Fe^{III}_8L_8]^{12+}$ (H_3L = tris{[2-{(imidazole-4-yl)methylid-ene}amino]ethyl}amine),[13] for which no magnetic data were reported, the spin crossover species $[\{Cu^{I}(Tp4py)(CH_3CN)\}_8\{Fe^{II}(NCS)_2\}_{10/3}\{Fe^{II}(NCS)(CH_3CN)\}_{8/3}](ClO_4)_{8/3}(CH_3CN)_n$ (Tp4py = tris{3-(4-pyridyl)-pyrazol-1-yl}hydroborate),[14] and in molecular Prussian blue species such as $[(Tp)_8(H_2O)_6Cu^{II}_6Fe^{III}_8(CN)_{24}]^{4+}$ (where Tp^- = hydrotris(pyrazolyl)borate).[15]

The direct current (d.c.) molar magnetic susceptibility, χ_M, of polycrystalline samples of complexes **1** and **2** were measured in an applied magnetic field, *B*, of 0.1 T, over the 5–280 K temperature, *T*, range (Figure 2, where $\chi = M/B$, and *M* is the magnetization). At 280 K, the $\chi_M T$ products of **1** and **2** have values of 17.7 and 26.3 $cm^3 mol^{-1} K$, respectively. These values are in excellent agreement with those expected from the spin-only contributions to the magnetism of a $[Cr^{III}_8Cu^{II}_6]$ unit (17.6 $cm^3 mol^{-1} K$), with $g_{Cr} = 2.00$ and $g_{Cu} = 2.15$, and of a $[Cr^{III}_8Co^{II}_6]$ unit (26.3 $cm^3 mol^{-1} K$), with $g_{Cr} = g_{Co} = 2.00$, where g_{Cr}, g_{Cu}, and g_{Co} are the *g*-factors of Cr^{III}, Cu^{II}, and Co^{II}, respectively. Upon cooling, the $\chi_M T$ product of **1** remains essentially constant down to 30 K, below which a fast increase is observed, reaching 19.1 $cm^3 mol^{-1} K$ at 5 K. This behavior is indicative of weak ferromagnetic exchange interactions. Upon cooling, the $\chi_M T$ product of **2** decreases continuously, reaching a plateau value of 21.5 $cm^3 mol^{-1} K$ at 8 K, before slightly increasing upon further cooling to 21.7 $cm^3 mol^{-1} K$ at 5 K. The analysis of this behavior is complicated by the combination of the ligand-field splitting of the Co^{II} ion and weak exchange interactions. The tetragonal symmetry ligand field of the {$Co(py)_4(H_2O)_2$} site removes the degeneracy of the $^4T_{1g}$ term, breaking it into ^4E_g and $^4A_{2g}$ terms, with the latter lower in energy.[16] Spin-orbit coupling (SOC) then further removes the degeneracy of the $^4A_{2g}$ term, breaking it into two Kramers doublets, the energy splitting of which can be parameterized as a zero-field splitting (*D*) of the $^4A_{2g}$ term. The fact that the high temperature $\chi_M T$ product of **2** agrees well with the expected spin-only value supports the dominance of the axial ligand field splitting over SOC.

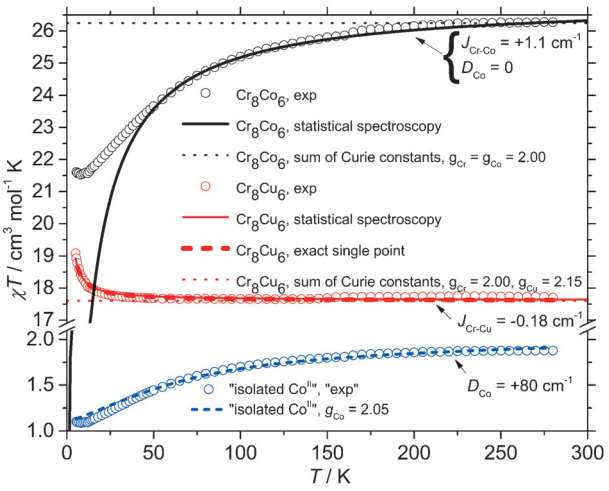

Figure 2. $\chi_M T$ products of **1** and **2**. The experimental data are shown as open circles. The curves obtained by statistical spectroscopy are shown as solid lines. The sums of the Curie constants of uncorrelated ions in **1** and **2** are shown as dotted lines. The results from matrix diagonalization of the blocked spin-Hamiltonian (1) for **1** and the best fit curve for "isolated Co^{II}", as explained in the text, for **2**, are shown as thick dashed lines.

For the quantitative interpretation of the magnetic properties of **1** and **2**, we used two limiting models: 1) with $D_M = 0$ and $J_{Cr\text{-}M} \neq 0$ (an isotropic model) and 2) with $J_{Cr\text{-}M} = 0$ and $D_M \neq 0$, where M = Cu^{II} or Co^{II}, and $J_{Cr\text{-}M}$ is the isotropic exchange parameter between Cr and M centers (where M = Cu for **1** and Co for **2**). In both limiting models, we neglected the single-ion anisotropy of Cr^{III}, D_{Cr}, as this is usually of the order of 1 cm^{-1}.[17] Given that $D_{Cu} = 0$, we only applied the isotropic model for the analysis of **1**. We started with the isotropic model for both **1** and **2**. To describe the magnetic properties we used the following isotropic spin-Hamiltonian (1)

$$\hat{H}_{iso} = J_{Cr-M} \sum_{\text{all Cr–M pairs}} \hat{S}_{Cr} \bullet \hat{S}_M + \mu_B B g \sum_i \hat{S}_{z,i} \qquad (1)$$

with *i* running over all constitutive metal centers, $\hat{S}$ a spin operator, μ_B the Bohr magneton, *B* the applied magnetic field, and *g* the isotropic *g*-factor common to both Cr and M. Modelling the data using traditional matrix diagonalization is impractical for **1** and impossible for **2**, because of the large

dimension (4,194,304 for **1** and 268,435,456 for **2**) of the associated spin-Hamiltonian matrices. The isotropic Heisenberg Hamiltonian (1) applied to these spin systems permits blocking of the spin-Hamiltonian matrix with respect to the total spin value, *S*. To model the magnetic properties of **1** and **2**, we have adapted computational techniques known in theoretical nuclear physics as statistical spectroscopy,[18] which exploit the moments of the Hamiltonian to calculate relevant thermodynamic properties. We calculated the temperature-dependent magnetic susceptibility of **1** and **2** by use of the van Vleck equation (2), derived from (1)

$$\chi = \frac{N_A g^2 \mu_B^2}{k_B T} \frac{\sum_S (2S+1)^{\frac{S(S+1)}{3}} \exp(-\frac{E_S}{k_B T})}{\sum_S (2S+1) \exp(-\frac{E_S}{k_B T})} \quad (2)$$

with N_A Avogadro's number, k_B the Boltzmann constant, and T the temperature. We approximated the energy dependence of the $(2S+1)$ factor in the denominator by a continuous density of states, $\rho(E)$. Similarly, we approximated the energy dependence of the $(2S+1)S(S+1)/3$ factor on the nominator, by a continuous density, $\rho_C(E)$, which we designated the Curie-constant density. These two densities may be obtained from moments of an appropriate Hamiltonian,[19] here (1). The moments are related to the traces of powers of the Hamiltonian.[19] The density $\rho(E)$ is determined from the moments of a Hamiltonian containing only the Heisenberg terms of (1), whereas the density $\rho_C(E)$ is determined from the bivariate moments of (1), that is, those obtained from a Hamiltonian containing both Heisenberg and Zeeman terms. Once these moments, up to order 14 in our case, had been computed, the densities were conveniently determined following the method described in references [20,21]. Using this approach, and by successive simulations of the temperature dependence of the $\chi_M T$ product of **1** and **2**, we determined $J_{Cr\text{-}Cu} = -0.18\ cm^{-1}$ with a common isotropic *g* factor $g_1 = 2.021$, for **1**, and $J_{Cr\text{-}Co} = +1.10\ cm^{-1}$ with a common isotropic *g*-factor $g_2 = 2.0$, for **2**. In our analysis, we neglected all Cr–Cr and M–M exchange interactions, because these centers are not connected as first neighbors. The results were in excellent agreement with experiment in the case of **1** (Figure 2). For **2**, they agreed well with the experimental data down to approximately 45 K. The observed deviation below this temperature could be attributed to the lack of anisotropy terms in (1). With these parameters, the ground spin state of **1** is an $S = 15$ state and the ground spin state of **2** would be an $S = 3$ state. To verify the validity of our theoretical approach, we calculated the $\chi_M T$ product of **1** by full matrix diagonalization of the blocked spin-Hamiltonian matrix of **1**, by use of the determined spin-Hamiltonian parameters. The resulting curve (Figure 2, thick dashed line) is in excellent agreement with the one obtained with the theoretical approach based on the moments of the spin-Hamiltonian.

In the analysis using model (2) for **2**, we assumed $J_{Cr\text{-}Co} = 0$. From the experimental $\chi_M T$ product of **2**, we subtracted the calculated $\chi_M T$ value ($15\ cm^3\,mol^{-1}\,K$) for eight uncoupled Cr^{III} ions (the small D_{Cr} parameter made no difference to the high temperature data), and divided the result by six, to generate the $\chi_M T$ curve for an "isolated" Co^{II} site (Figure 2). We then attempted to fit the $\chi_M T$ product of the "isolated" Co^{II} site to an anisotropic single-ion spin-Hamiltonian:

$$\hat{H}_{aniso} = D_{Co}\left[\hat{S}^2_{z,Co} - S_{Co}(S_{Co}+1)/3\right] + \mu_B B g_{Co} \hat{S}_{Co} \quad (3)$$

with $S_{Co} = 3/2$, reflecting the $^4A_{2g}$ ground term of Co^{II}. A reasonable, but not perfect, agreement was found for $g_{Co} = 2.0$ and $D_{Co} = +80\ cm^{-1}$ (Figure 2). With these parameters, only the ground ($|m| = {}^1/_2$) Kramers doublet would be populated at low temperatures. Given that the observed low-temperature $\chi_M T$ value for an "isolated" Co^{II} is of the order of $1.1\ cm^3\,K\,mol^{-1}$, the calculated low-temperature paramagnetic $\chi_M T$ limit for **2** would be about $21.6\ cm^3\,K\,mol^{-1}$, in good agreement with the observed low-temperature plateau value of $21.5\ cm^3\,mol^{-1}\,K$, at 8 K.

The nature of the weak exchange interactions in **1** and **2** was further probed by Q- and W-band EPR spectroscopy (34 and 94 GHz, respectively). Spectra of $[Cr^{III}L_3]$, that is, the isolated corner fragment of **1** and **2** at 5 K are those of an $S_{Cr} = 3/2$ ($g_{Cr} = 1.97$) with near axial ZFS parameters of $D_{Cr} = -0.55$ and $E_{Cr} = 0.025\ cm^{-1}$, in the range found for other [Cr(diketonate)$_3$] complexes[17] (Figures S5 and S3; simulated[22] with a Gaussian linewidth of 60 mT and a 10% D-strain).

Spectra of **1** at 5 K are severely broadened compared with $[Cr^{III}L_3]$, with linewidths approaching 400 mT (Figure S6), consistent with $|J_{Cr\text{-}Cu}|$ being smaller than $|D_{Cr}|$ and with an upper bound given by the linewidth; also consistent with $J_{Cr\text{-}Cu}$ as determined from statistical spectroscopy methods. The lack of structure prevents any further analysis. Spectra of **2** are also broadened but structured (Figure 3), resembling those of $[Cr^{III}L_3]$ with noticeable shifts in resonance fields and new resonances at around 1400 mT (at W-band) because of the Co^{II} sites. This implies $|J_{Cr\text{-}Co}| < |D_{Co}|$. The matrix dimension of **2** is far too large for simulation using the full Cr_8Co_6 spin system, while the weak exchange limit precludes handling the problem by low-energy subspace methods.[23] Hence, we attempted to model the spectra of **2** as a simple $Cr^{III}Co^{II}$ dimer, of which the parameters for Cr^{III} are defined experimentally from $[Cr^{III}L_3]$, and those for Co^{II} are fixed from the "isolated" $S_{Co} = 3/2$ Co^{II} model (Figure 2). We also fixed the relative orientation of the principal axes of the D_{Cr} and D_{Co} ZFS tensors to 54.7°, which is the angle between the C_4 (face-normal, defining the unique axis of Co^{II} in **2**) and C_3 (body-diagonal, defining the unique axis of Cr^{III} in **2**) axes of a cube. Thus, the only variable is $J_{Cr\text{-}Co}$. The calculated spectra were very sensitive to small $J_{Cr\text{-}Co}$ (e.g. Figure S7), and we could reproduce the experimental resonances reasonably with $J_{Cr\text{-}Co} = -0.3\ cm^{-1}$ (Figure 3, bottom, and S7). Note that the determined $J_{Cr\text{-}Co}$ value is not that of **2** but for the fictitious $Cr^{III}Co^{II}$ dimer. The isotropic exchange parameter, $J_{Cr\text{-}Co}$, of **2** is likely smaller in magnitude.

Variable-temperature-and-variable-field (VTVB) magnetization studies of complexes **1** and **2** (Figure S8) were consistent with weak exchange in both cases. For **1**, the saturation magnetic moment of 30.8 μ_B at 5 T and 2 K, was as expected for full spin alignment. In the case of **2**, the magnetic moment was also 30.8 μ_B at 5 T and 2 K. If only the lower Kramers doublet of Co^{II} (which has $g_{eff,x} = 4$, $g_{eff,y} = 4$, $g_{eff,z} = 2$)

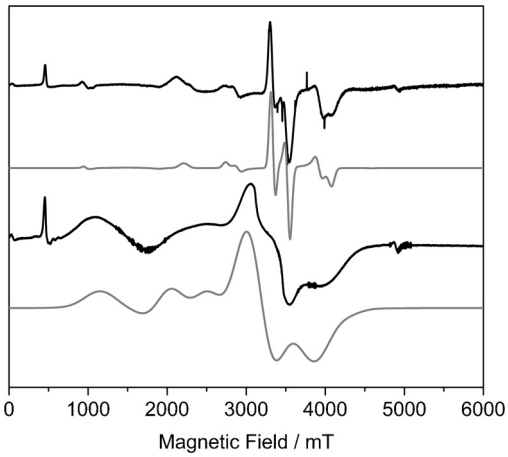

Figure 3. W-band EPR spectra of $[Cr^{III}L_3]$ (top) and **2** (bottom) in the solid state and 5 K (black lines). Calculated spectra (grey lines) 1) for $S_{Cr}=3/2$, $g_{Cr}=1.97$, $D_{Cr}=+0.55$ and $E_{Cr}=0.025$ cm^{-1} (top), and 2) for a $Cr^{III}Co^{II}$ dimer, with $S_{Cr}=S_{Co}=3/2$, $g_{Cr}=1.97$, $g_{Co}=2.05$, $D_{Cr}=-0.55$ cm^{-1}, $E_{Cr}=0.025$ cm^{-1}, $D_{Co}=+80$ cm^{-1}, $J_{Cr\text{-}Co}=-0.3$ cm^{-1} and an angle between the D_{zz}^{Cr} and D_{zz}^{Co} vectors of 54.7° (bottom; 400 mT Gaussian linewidth).

is populated in this regime ($D_{Co} \gg kT$), then the theoretical maximum magnetization is 34 μ_B, in reasonable agreement with the experimental data, given the simplicity of the model.

The flexibility in the design and construction of these $[M^{III}{}_8M^{II}{}_6]^{12+}$ cages offers enormous scope for tuning their physical properties. The corner ions can potentially be any M^{III} ion, as long as the precursor ML_3 can be prepared; the face-capping metal ions can be any M^{II} ion that can adopt square-planar, square-pyramidal, or octahedral geometry. The 12+ charge on the cage suggests that the anions can be varied and can be innocent or non-innocent, and the solvent bonded terminally to the M^{II} ions should be easily replaced, thus allowing the attachment of a host of different species and/or the assembly of the cubes into higher-order structures. The large internal cavity suggests that the cage could play host to different species, and indeed one can imagine constructing magnetic coordination capsules capable of hosting magnetic and/or redox-active guests, exerting control over (switching on and off) magnetic exchange between metal ions in the host framework and between the host and guest(s). Post-synthetic exohedral functionalization and simple changes to ligand design will also allow the modification of the magnetic properties, but additionally can be manipulated to tune solubility, reactivity, stability, and substrate specificity.

Keywords: EPR spectroscopy · heterometallic cages · magnetometry · molecular magnetism · transition metals

How to cite: *Angew. Chem. Int. Ed.* **2015**, *54*, 6761–6764
Angew. Chem. **2015**, *127*, 6865–6868

[1] S. Thiele, F. Balestro, R. Ballou, S. Klyatskaya, M. Ruben, W. Wernsdorfer, *Science* **2014**, *344*, 1135.
[2] M. Ganzhorn, S. Klyatskaya, M. Ruben, W. Wernsdorfer, *Nat. Nanotechnol.* **2013**, *8*, 165.
[3] G. A. Timco, E. J. L. McInnes, R. E. P. Winpenny, *Chem. Soc. Rev.* **2013**, *42*, 1796.
[4] A. Cornia, M. Mannini, P. Sainctavit, R. Sessoli, *Chem. Soc. Rev.* **2011**, *40*, 3076.
[5] G. Aromí, D. Aguila, P. Gamez, F. Luis, O. Roubeau, *Chem. Soc. Rev.* **2012**, *41*, 537.
[6] J. Lehmann, A. Gaita-Ariño, E. Coronado, D. Loss, *Nat. Nanotechnol.* **2007**, *2*, 312.
[7] a) G. Aromí, E. K. Brechin, *Struct. Bonding (Berlin)* **2006**, *122*, 1; b) C. J. Milios, R. E. P. Winpenny, *Struct. Bond.* **2014**, DOI: 10.1007/430_2014_149; c) J.-N. Rebilly, T. Mallah, *Struct. Bonding (Berlin)* **2006**, *122*, 103–131.
[8] a) T. Murase, Y. Nishijima, M. Fujita, *J. Am. Chem. Soc.* **2012**, *134*, 162–164; b) C. Zhao, Q.-F. Sun, W. M. Hart-Cooper, A. G. DiPasquale, F. D. Toste, R. G. Bergman, K. N. Raymond, *J. Am. Chem. Soc.* **2013**, *135*, 18802–18805; c) F. Schmitt, J. Freudenreich, N. P. E. Barry, L. Juillerat-Jeanneret, G. Süss-Fink, B. Therrien, *J. Am. Chem. Soc.* **2012**, *134*, 754–757; d) P. Mal, B. Breiner, K. Rissanen, J. R. Nitschke, *Science* **2009**, *324*, 1697–1699.
[9] M. M. J. Smulders, A. Jiménez, J. R. Nitschke, *Angew. Chem. Int. Ed.* **2012**, *51*, 6681–6685; *Angew. Chem.* **2012**, *124*, 6785–6789.
[10] a) S. Hiraoka, Y. Sakata, M. Shionoya, *J. Am. Chem. Soc.* **2008**, *130*, 10058–10059; b) S.-L. Huang, Y.-J. Lin, T. S. A. Hor, G.-X. Jin, *J. Am. Chem. Soc.* **2013**, *135*, 8125–8128; c) H. Li, Y.-F. Han, Y.-J. Lin, Z.-W. Guo, G.-X. Jin, *J. Am. Chem. Soc.* **2014**, *136*, 2982–2985; d) A. J. Metherell, M. D. Ward, *Chem. Commun.* **2014**, *50*, 6330; e) H.-B. Wu, Q.-M. Wang, *Angew. Chem. Int. Ed.* **2009**, *48*, 7343; *Angew. Chem.* **2009**, *121*, 7479; f) M. B. Duriska, S. M. Neville, B. Moubaraki, J. D. Cashion, G. J. Halder, K. W. Chapman, C. Balde, J.-F. Létard, K. S. Murray, C. J. Kepert, S. R. Batten, *Angew. Chem. Int. Ed.* **2009**, *48*, 2549; *Angew. Chem.* **2009**, *121*, 2587; g) M. B. Duriska, S. M. Neville, J. Lu, S. S. Iremonger, J. F. Boas, C. J. Kepert, S. R. Batten, *Angew. Chem. Int. Ed.* **2009**, *48*, 8919; *Angew. Chem.* **2009**, *121*, 9081; h) J. L. Heinrich, P. A. Berseth, J. R. Long, *Chem. Commun.* **1998**, 1231.
[11] a) S. Mecozzi, J. Rebek, *Chem. Eur. J.* **1998**, *4*, 1016; b) N. R. Voss, M. Gerstein, *Nucleic Acids Res.* **2010**, *38*, W555.
[12] H.-B. Wu, Q.-M. Wang, *Angew. Chem. Int. Ed.* **2009**, *48*, 7343; *Angew. Chem.* **2009**, *121*, 7479.
[13] F. Reichel, J. K. Clegg, K. Gloe, J. J. Weigand, J. K. Reynolds, C.-G. Li, J. R. Aldrich-Wright, C. J. Kepert, L. F. Lindoy, H.-C. Yao, F. Li, *Inorg. Chem.* **2014**, *53*, 688.
[14] M. B. Duriska, S. M. Neville, B. Moubaraki, J. D. Cashion, G. J. Halder, K. W. Chapman, C. Balde, J.-F. Létard, K. S. Murray, C. J. Kepert, S. R. Batten, *Angew. Chem. Int. Ed.* **2009**, *48*, 2549; *Angew. Chem.* **2009**, *121*, 2587.
[15] See for example a) J. J. Sokol, M. P. Shores, J. R. Long, *Angew. Chem. Int. Ed.* **2001**, *40*, 236; *Angew. Chem.* **2001**, *113*, 242; b) S. Wang, J.-L. Zuo, H.-C. Zhou, H. J. Choi, Y. Ke, J. R. Long, X.-Z. You, *Angew. Chem. Int. Ed.* **2004**, *43*, 5940; *Angew. Chem.* **2004**, *116*, 6066.
[16] L. L. Lohr, J. C. Miller, R. R. Sharp, *J. Chem. Phys.* **1999**, *111*, 10148; A. Bencini, C. Benelli, D. Gatteschi, C. Zanchini, *Inorg. Chem.* **1980**, *19*, 1301.
[17] G. Elbers, S. Remme, G. Lehmann, *Inorg. Chem.* **1986**, *25*, 896.
[18] S. S. M. Wong, *Nuclear Statistical Spectroscopy*, Oxford University Press and Clarendon Press, Oxford, **1986**.
[19] G. S. Rushbrooke, P. J. Wood, *Mol. Phys.* **1958**, *1*, 257.
[20] a) L. R. Mead, N. Papanicoaou, *J. Math. Phys.* **1984**, *25*, 2404; b) S. M. Grimes, T. N. Massey, *Fusion Eng. Des.* **1997**, *37*, 89.
[21] S. M. Grimes, T. N. Massey, *Phys. Rev. C* **1995**, *51*, 606.
[22] Simulations performed with EasySpin software: S. Stoll, A. Schweiger, *J. Magn. Reson.* **2006**, *178*, 42.
[23] S. Piligkos, E. Bill, D. Collison, E. J. L. McInnes, G. A. Timco, H. Weihe, R. E. P. Winpenny, F. Neese, *J. Am. Chem. Soc.* **2007**, *129*, 760.

Received: February 3, 2015
Published online: April 20, 2015

